Conformation Analysis

DOI: 10.1002/anie.201402863

Dynamics of Intact Immunoglobulin G Explored by Drift-Tube Ion-Mobility Mass Spectrometry and Molecular Modeling**

*Kamila J. Pacholarz, Massimiliano Porrini, Rachel A. Garlish, Rebecca J. Burnley, Richard J. Taylor, Alistair J. Henry, and Perdita E. Barran**

Abstract: *Collision cross-sections (CCS) of immunoglobulins G1 and G4 have been determined using linear drift-tube ion-mobility mass spectrometry. Intact antibodies and Fc-hinge fragments present with a larger range of CCS than proteins of comparable size. This is rationalized with MD simulations, which indicate significant in vacuo dynamics between linked folded domains. The IgG4 subclass presents over a wider CCS range than the IgG1 subclass.*

Immunoglobulins (Ig), also known as antibodies, are glycoproteins employed by the immune system to identify and neutralize foreign objects. Antibodies and related products form the fastest growing class of therapeutic agents, with increasing application in the treatment of diseases including cancer, immunological and neurodegenerative disorders, and other pathologies. In the past three decades, more than 40 monoclonal antibodies (mAbs) and their derivatives have been approved for use in various indications, and currently many more are in research and pre-clinical trials.[1,2] Between 2006 and 2010, 13 new mAbs were approved as therapeutics, representing over a half of genuinely new biopharmaceuticals to come on market in that period.[3] Being far larger, more heterogenic, and produced as a result of batch processing, protein-based drugs provide a significant regulatory challenge compared to small molecules.

[*] Prof. P. E. Barran
MIB & School of Chemistry, The University of Manchester
131 Princess Street, Manchester M1 7DN (UK)
E-mail: perdita.barran@manchester.ac.uk
K. J. Pacholarz
The EastChem School of Chemistry, University of Edinburgh
West Mains Road, EH9 3JJ, Edinburgh (UK)
Dr. M. Porrini
Institute Européen de Chimie et Biologie (IECB), CNRS UMR 5248
Chimie et Biologie des Membranes et des Nano-objets (CBMN)
2 rue Robert Escarpit, 33607 Pessac Cedex (France)
Dr. R. A. Garlish, Dr. R. J. Burnley, Dr. R. J. Taylor, Dr. A. J. Henry
UCB Pharma
216 Bath Road, Slough SL1 3WE (UK)

[**] This work has been funded by the award of an MRC Industrial Case Studentship to K.J.P. in collaboration with UCB Pharma. We are truly grateful to Dr. Michel Laguerre for allowing us to run all of the MD simulations using the computational resources of his research group, located at the European Institute of Chemistry and Biology, Pessac (France). We thank Dr. Shirley Peters for providing us with the IgG samples.

Supporting information for this article is available on the WWW under http://dx.doi.org/10.1002/anie.201402863.

Regulatory authorities have identified three characteristics of a protein biopharmaceutical critical for development: post-translational modifications (PTMs), three-dimensional structure, and protein aggregation.[4,5] A method of characterization that could satisfy all of those needs is mass spectrometry.[5,6] For the latter two characteristics, the hybrid technique of ion mobility mass spectrometry (IM-MS), which facilitates study of protein higher-order structure, is particularly appropriate. IM-MS provides shape-defining parameters for each mass- (and charge)-selected species, termed their collision cross-sections (CCS). Moreover, as IM-MS provides data on isolated molecules, it can delineate structural changes that occur upon ligand binding or environmental change, which can be compared with theoretical values derived from structures found with other methods.

Immunoglobulins are classified by structural features, which in turn affect their function. Herein, we consider the G isotype (IgG), commonly used as a template for therapeutics design. IgGs are circa 150 kDa heteromeric protein complexes composed of four subunits: two identical heavy chains are linked by disulfide bonds, which are also connected to two light chains, resulting in a covalent tetramer with two identical halves commonly depicted as a "Y" shape. Each of the four chains contains a variable domain that is responsible for the specificity of antigen binding. Furthermore, IgGs are divided into subclasses (IgG1, IgG2, IgG3, and IgG4) based on the number and properties of connections in-between chains in the hinge region. IM-MS has 1) resolved conformers of intact IgG2 due to different disulphide bond formation in the hinge region;[7,8] 2) been used to investigate interactions between protein standards and commercially available antibodies commonly used in ELISA[9] tests; and 3) been applied to monitor Fab arm exchange and the formation of bispecific mAbs.[10] We employ drift tube ion mobility mass spectrometry (DT IM-MS) and molecular dynamics (MD) simulations to investigate two IgG1 and two IgG4 molecules of different antigen specificity.

Our in-house modified ion-mobility mass spectrometer allows the direct measurement of rotationally averaged helium CCS[11] (see the Supporting Information for further details). Two types of IgG1 and IgG4 antibodies denoted here as A and B are examined. Nano-electrospray mass spectra (nESI-MS) of 5 μM IgG1 A and IgG4 A in 100 mM ammonium acetate are shown in Figure 1, showing narrow charge state distributions diagnostic of "native"-like nESI-MS conditions. Both IgG subclasses, IgG1 and IgG4, have nearly the same molecular mass, and are not distinguishable by this mass

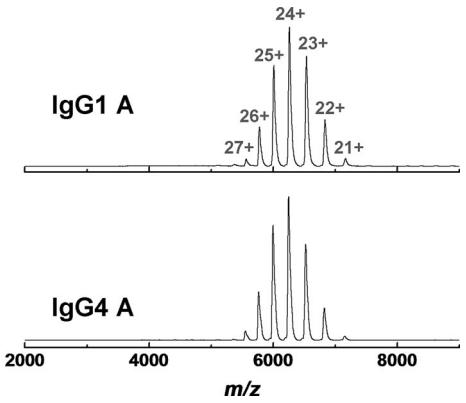

Figure 1. Mass spectra of IgG1 A (top) and IgG4 A (bottom) in 100 mM ammonium acetate. Peaks corresponding to intact IgG are observed in the circa 5700–7200 m/z range; the charge state envelope ranging from 21+ to 27+ is centered at 24+ charge state. Mass spectra of IgG1 B and IgG4 B are shown in the Supporting Information, Figure S1.

spectrometry analysis; resolution in excess of 100000 would be required.

Arrival time distributions (ATDs) were recorded following mobility separation and converted into CCS distributions (CCSDs; Figure 2; see the Supporting Information for details). Across the four antibodies investigated, all present very broad ATDs describing CCS landscapes populated from about 50 to 100 nm^2. Figure 2 shows CCSD obtained for the most populated charge states ($z = 22+$ to 26+) for IgG1 A and IgG4 A species (for IgG1 B and IgG4 B data, see the Supporting Information; Figure S2). Median CCS values from the total occupied space for each charge state are given in the Supporting Information, Table S1. Whilst the trends for each antibody are similar, the range of CCS presented over the charge states observed differ (Figure 2 and Table S1).

For the lowest charge state (22+) the median CCS found for IgG1 and IgG4 are the same (ca. 61–62 nm^2) as is the width of the ATD, suggesting indistinguishable conformations. As the charge state increases, so does the CCS for each mAb. For the two highest charge states of significant intensity, the observed CCS for IgG4 molecules are larger than the equivalent for the IgG1 mAbs. The change in median CCS across the charge state range is 15 nm^2 for both IgG1s and 20 nm^2 for both IgG4s, and thus the conformers adopted by the different isotypes of mAb appear distinguishable by IM-MS.

CryoEM and TEM studies have indicated that IgGs are flexible dynamic molecules, capable of Fab arm-waving and rotation, as well as Fab elbow-bending or Fc wagging.[12] Mean Fab-Fab angles have been previously reported (117 ± 43° for IgG1 and 128 ± 39° for IgG4);[13] the large standard deviations on these values is attributed to a high degree of flexibility. Considering this, we attribute the wide CCSD to a large number of probably closely related conformational families present in the gas phase with dynamic flexibility that cannot be resolved by room temperature ion mobility measurements. Whilst some features (notably the tail on the LHS for the 26+ species) suggest different conformations under each charge state, the lack of baseline resolution means that we can only surmise that the mAbs present interconverting conformers.

We have compared the conformational spread we observe for mAbs to that we have found for similarly sized protein complexes in terms of molecular mass (Figure 3). As

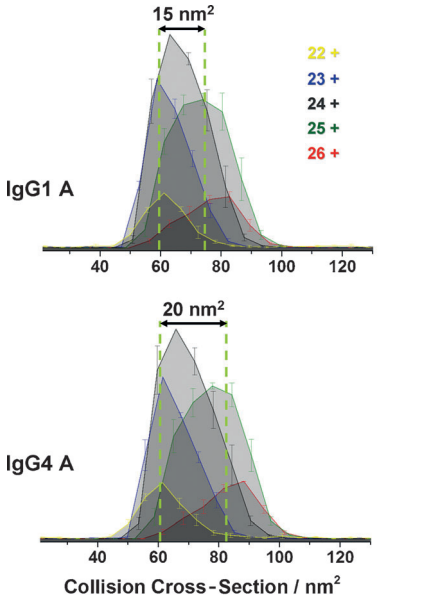

Figure 2. Conformational space occupied by IgG1 A and IgG4 A (149 kDa) for each charge state, in collision cross-sections (CCS). Data shown was acquired at 300 K and at a fixed drift voltage of 35 V and has been normalized to spectral intensity. Different solution conditions were investigated to optimise nESI (see the Supporting Information, Figures S3, S4).

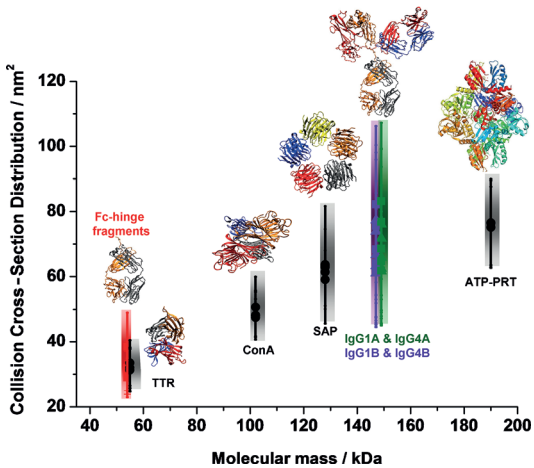

Figure 3. Collision cross-section distributions (CCSD) of the detected charge states versus molecular mass of Fc-hinge fragments, transthyretin (TTR, PDB:1BMZ), concanavalin A (ConA, PDB:1DQ0), human serum amyloid P component (SAP, PDB:1SAC), IgG1 and IgG4 (PDB:1IGY), and MtATP-phosporibosyltransferase (ATP-PRT, PDB:1NH7) along with structures based on crystal data deposited into the protein data bank. The lines represent CCSD width; ▲ IgG1 subclass, ■ IgG4 subclass.

expected, absolute CCS increase with increasing protein mass; however, IgGs display a notably wider range of conformations, which we attribute to dynamic flexible structures. Whilst the 24+ IgG species with a median CCS of ca. 67 nm^2 follows a trend line set by other multimeric protein complexes, for example transthyretin (TTR ca. 55 kDa, ca. 30.5 nm^2), concanavalin A (ConA ca. 102 kDa, 47.4 nm^2), and human serum amyloid P component (hSAP ca. 128 kDa, 60.5 nm^2), the higher charge states ($z > 24$) deviate significantly. These trends can also be observed by comparing the CCSD of each protein. Intact IgG1 and IgG4 molecules present wider CCSD, populating more conformational space than other multimeric complexes of similar masses (Supporting Information, Figures S5–S7).

The hinge region of the IgG1 subclass is more flexible in comparison to the hinge of the IgG4 subclass.[13–15] The structure and stability of IgG antibodies has been shown to be affected by differences in the inter- and intra-disulfide bonds. The non-classical structure of the IgG2 B (where both Fab arms have interchain disulfide bonds to the hinge region) has been shown to be more compact than that of IgG2 A (where neither of Fab arms are linked to the hinge) by SEC and AUC.[16] These isoforms have previously been resolved with IM-MS.[7] Moreover, disulfide linkages between light and heavy chain vary among the IgG subclasses, resulting in structural differences. This bond links the carboxy terminal of the light chain with the cysteine residue at position 220 (in IgG1) and at position 131 (in IgG2, IgG3, and IgG4) of the CH1 sequence of the heavy chain. We speculate that the light chain of IgG4 (as well as IgG2 and IgG3), being linked further from the center of mass, will allow for more movement, and having more accesible space, could present broader total CCSD, as shown experimentally (Figure 2).

Fc-hinge fragments display narrow charge state distribution centered at the 13+ charge state (Supporting Information, Figures S8 and S9) but for both IgG1 and IgG4 also present broad CCSD compared to similarily sized proteins (Figure 3). No striking differences in CCSD have been noted for the 12+ and 13+ charge states. The highest charge state, 14+, of IgG4 displays two conformational families, with the larger one centered at 36.5 nm^2 being more abundant as opposed to the Fc-hinge fragment of IgG1, with the majority of species centered at 31.6 nm^2. Distinct features in the hinge region and non-covalent interactions in the CH3–CH3 domains are potentially responsible for the experimentally observed differences.[17,18] These and/or other interactions may dictate how the intrinsic flexibility varies.

Full structural characterization of antibodies has been hindered by their flexibility.[13,19] Most of the hundreds of IgG structures available at the protein data bank (PDB) are merely fragments of antibodies: typically just the Fab arm with the specific binding pocket or the Fc domains. There are to date just three X-ray crystallography-based structures of intact IgGs deposited: human IgG1 b12 (1HZH), IgG2a (1IGT), and IgG1 (1IGY).[20–22] To provide further insight to experimental results, we performed in vacuo molecular dynamic (MD) simulations starting from the crystal structures. We discounted 1HZH, as the deposited co-ordinates have residues missing including some in the hinge region. The antibodies were first gradually heated up to 300 K, and then subjected to molecular dynamics (MD) run of 10 ns (Figure 4; Supporting Information, S10). We report the conformation change with respect to simulation time in terms of the CCS of each mAb using three approximations: the projection approximation (PA),[23] the trajectory method (TM),[24] and the exact hard sphere scattering (EHS)[25] (Supporting Information, Table S2). The most robust method is TM, and we only discuss results from that here. At $t = 0$, theoretical CCS calculated with the trajectory method are found to be 105.6 nm^2 and 100.8 nm^2 for 1IGT and 1IGY, respectively. Experimentally determined CCS are significantly lower, indicating that the protein has collapsed somewhat in comparison to the X-ray structure. MD simulations support this observation; over only 10 ns of dynamics, each antibody undergoes a significant compaction. After 10 ns of in vacuo MD simulations, theoretical CCS calculated with the trajectory method decreased to 86.5 nm^2 and 84.1 nm^2 for 1IGT and 1IGY, respectively. These CCS are still a little higher than median experimental values, although Figure 2 shows that around 20% of the conformational occupancy of the mAbs is at or above these $t = 10$ ns theoretical values. As the millisecond timescale of the ion mobility experiments greatly exceeds the simulation time, we can predict further structural compaction with longer time in vacuo. Moreover, it is worth noting that for each antibody, the CCS do not simply decrease as the simulation time progresses but fluctuate, which is indicative of flexible molecules presenting many interconverting conformers. This conclusion is also supported by wide

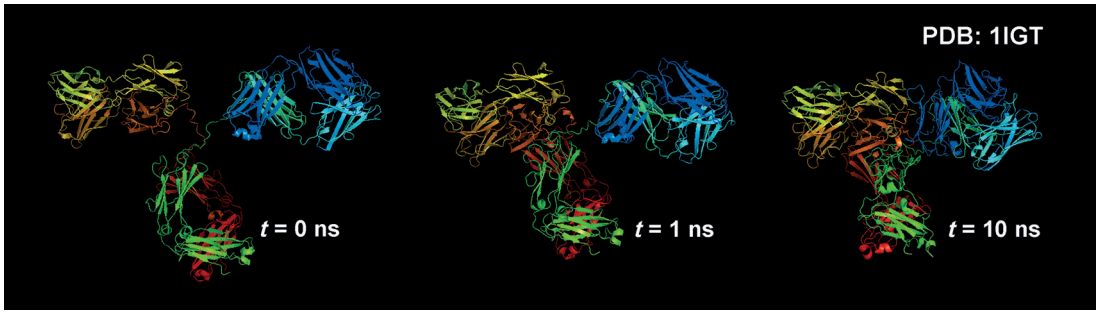

Figure 4. In vacuo molecular dynamic simulations on IgG2a (PDB:1IGT). Structural collapse can be mainly observed around the hinge region. Theoretical CCS can be found in the Supporting Information, Table S2 and Figure S10.

Table 1: Secondary structure content and theoretical CCS (trajectory method TM) of 1IGT prior to and at 2 ns intervals of in vacuo MD simulation.[a]

Simulation time [ns]	0	2	4	6	8	10
TM Collision cross-section [nm^2]	106	89	87	86	89	86
Coil/turn	34.42/11.25	37.92/11.32	39.82/10.79	42.48/11.63	40.20/10.87	41.95/10.11
Parallel-β-sheet	2.13	2.05	2.13	1.52	1.98	1.67
Anti-parallel-β-sheet	45.14	41.64	40.88	39.29	41.11	40.05
3_{10}-helix	3.50	3.57	3.80	2.66	3.50	3.80
α-helix	3.57	3.12	3.20	2.05	1.82	2.28
$\pi_{(3\text{-}14)}$-helix	0.00	0.38	0.38	0.38	0.53	0.15

[a] Data for the PDB:1IGY structure is available in the Supporting Information, Table S3.

ATDs and the corresponding large CCSD across the narrow charge state range compared with that found for other proteins (Figure 3; Supporting Information, Figures S6, S7).

The solvent content, from the Matthews coefficient, for the PDB structures 1IGY and 1IGT is 59% and 64%, respectively.[26] In each case, this is higher than the average protein crystal structure solvent content of about 47% (calculated from 10471 entities).[27] As the mAbs desolvate, they lose both solvent and stabilizing buffer interactions; based on the high solvent content of the unit cells used here as a comparison, we would predict a contraction as we observe. Whilst these are not identical to the mAb studied experimentally, structural homology allows us to predict which regions of an mAb will contract and also which are unchanged in vacuo. Despite a significant change in the theoretical CCS, the secondary structure content does not change drastically (Tables 1 and S3). After 10 ns of in vacuo MD simulation of the 1IGT crystal structure, the total helical content decreases from 7.1% to 6.2% and the total β-sheet content decreases from 47.2% to 41.7%. It can be seen in Figure 4 that structural contraction occurs mainly around the hinge region and that the antigen binding region is still well-preserved. The linked folded domains proteins "dance" in the absence of solution as they do in the condensed phase.[13–15]

In summary, IM-MS has shown intact mAbs to be more conformationally diverse than proteins of comparable size, which we attribute to intrinsic flexibility. The wide CCSD compared to other proteins suggest that the conformational dynamics (dancing) is post-desolvation, but that the sampled species sorted by charge arise from non-identical conformational ensembles in solution. There is some collapse of the MD structures and some extension; this all happens at very low net charge states where we would not expect significant columbic repulsion. MD simulations indicate that desolvation causes a contraction in the hinge region and loss of the cavities between domains; however, despite this the IgGs still retain much of the secondary structure as well as the tertiary fold. We report subtle differences in IM-MS data from the two IgG subclasses, with IgG1 less flexible than IgG4 in the absence of solvent; this contrasts with solution findings which have reported the IgG4 hinge as more rigid than that of IgG1, and raises interesting caveats about the use of mass spectrometry to probe higher-order structure in flexible proteins.

Received: February 27, 2014
Revised: April 7, 2014
Published online: June 10, 2014

Keywords: conformation analysis · immunoglobulin G · mass spectrometry · molecular dynamics · protein structures

[1] A. Beck, T. Wurch, C. Bailly, N. Corvaia, *Nat. Rev. Immunol.* **2010**, *10*, 345 – 352.
[2] J. M. Reichert, *Mabs* **2010**, *2*, 84 – 100.
[3] G. Walsh, *Nat. Biotechnol.* **2010**, *28*, 917 – 924.
[4] S. A. Berkowitz, J. R. Engen, J. R. Mazzeo, G. B. Jones, *Nat. Rev. Drug Discovery* **2012**, *11*, 527 – 540.
[5] A. Beck, E. Wagner-Rousset, D. Ayoub, A. Van Dorsselaer, S. Sanglier-Cianferani, *Anal. Chem.* **2013**, *85*, 715 – 736.
[6] N. J. Thompson, S. Rosati, R. J. Rose, A. J. R. Heck, *Chem. Commun.* **2013**, *49*, 538 – 548; V. Richter, M. Kwiatkowski, M. Omidi, W. D. Robertson, H. Schlueter, *Pharm. Bioprocess.* **2013**, *1*, 381 – 404.
[7] D. Bagal, J. F. Valliere-Douglass, A. Balland, P. D. Schnier, *Anal. Chem.* **2010**, *82*, 6751 – 6755.
[8] L. M. Jones, H. Zhang, W. Cui, S. Kumar, J. B. Sperry, J. A. Carroll, M. L. Gross, *J. Am. Soc. Mass Spectrom.* **2013**, *24*, 835 – 845.
[9] C. Pritchard, G. O'Connor, A. E. Ashcroft, *Anal. Chem.* **2013**, *85*, 7205 – 7212.
[10] F. Debaene, E. Wagner-Rousset, O. Colas, D. Ayoub, N. Corvaïa, A. Van Dorsselaer, A. Beck, S. Cianférani, *Anal. Chem.* **2013**, *85*, 9785 – 9792.
[11] B. J. McCullough, J. Kalapothakis, H. Eastwood, P. Kemper, D. MacMillan, K. Taylor, J. Dorin, P. E. Barran, *Anal. Chem.* **2008**, *80*, 6336 – 6344.
[12] O. H. Brekke, T. E. Michaelsen, I. Sandlie, *Immunol. Today* **1995**, *16*, 85 – 90.
[13] K. H. Roux, L. Strelets, T. E. Michaelsen, *J. Immunol.* **1997**, *159*, 3372 – 3382.
[14] V. T. Oi, T. M. Vuong, R. Hardy, J. Reidler, J. Dangl, L. A. Herzenberg, L. Stryer, *Nature* **1984**, *307*, 136 – 140.
[15] J. L. Dangl, T. G. Wensel, S. L. Morrison, L. Stryer, L. A. Herzenberg, V. T. Oi, *EMBO J.* **1988**, *7*, 1989 – 1994.
[16] T. M. Dillon, M. S. Ricci, C. Vezina, G. C. Flynn, Y. D. Liu, D. S. Rehder, M. Plant, B. Henkle, Y. Li, S. Deechongkit, B. Varnum, J. Wypych, A. Balland, P. V. Bondarenko, *J. Biol. Chem.* **2008**, *283*, 16206 – 16215.
[17] T. Rispens, P. Ooievaar-De Heer, E. Vermeulen, J. Schuurman, M. v. d. N. Kolfschoten, R. C. Aalberse, *J. Immunol.* **2009**, *182*, 4275 – 4281.
[18] A. F. Labrijn, T. Rispens, J. Meesters, R. J. Rose, T. H. den Bleker, S. Loverix, E. T. J. van den Bremer, J. Neijssen, T. Vink, I. Lasters, R. C. Aalberse, A. J. R. Heck, J. G. J. van de Winkel, J. Schuurman, P. W. H. I. Parren, *J. Immunol.* **2011**, *187*, 3238 – 3246.
[19] L. Bongini, D. Fanelli, F. Piazza, P. De Los Rios, S. Sandin, U. Skoglund, *Proc. Natl. Acad. Sci. USA* **2004**, *101*, 6466 – 6471.
[20] E. O. Saphire, P. Parren, R. Pantophlet, M. B. Zwick, G. M. Morris, P. M. Rudd, R. A. Dwek, R. L. Stanfield, D. R. Burton, I. A. Wilson, *Science* **2001**, *293*, 1155 – 1159.

[21] L. J. Harris, E. Skaletsky, A. McPherson, *J. Mol. Biol.* **1998**, *275*, 861 – 872.
[22] L. J. Harris, S. B. Larson, K. W. Hasel, A. McPherson, *Biochemistry* **1997**, *36*, 1581 – 1597.
[23] T. Wyttenbach, G. vonHelden, J. J. Batka, D. Carlat, M. T. Bowers, *J. Am. Soc. Mass Spectrom.* **1997**, *8*, 275 – 282.
[24] M. F. Mesleh, J. M. Hunter, A. A. Shvartsburg, G. C. Schatz, M. F. Jarrold, *J. Phys. Chem.* **1996**, *100*, 16082 – 16086.
[25] A. A. Shvartsburg, M. F. Jarrold, *Chem. Phys. Lett.* **1996**, *261*, 86 – 91.
[26] B. W. Matthews, *J. Mol. Biol.* **1968**, *33*, 491 – 497.
[27] K. A. Kantardjieff, B. Rupp, *Protein Sci.* **2003**, *12*, 1865 – 1871.

